Mon. Not. R. Astron. Soc. **269**, 998–1010 (1994)

New identifications and redshifts for southern 2-Jy radio sources

S. di Serego Alighieri,[1] I. J. Danziger,[2] R. Morganti[3]† and C. N. Tadhunter[4]
[1] *Osservatorio Astrofisico di Arcetri, L.go E. Fermi 5, I-50125 Firenze, Italy*
[2] *ESO, Karl-Schwarzschild-Strasse-2, D-85748, Garching bei München, Germany*
[3] *Istituto di Radioastronomia, via Irnerio 46, I-40126 Bologna, Italy*
[4] *Department of Physics, University of Sheffield, Sheffield S3 7RH*

Accepted 1994 March 24. Received 1994 March 7

ABSTRACT
We present new optical identifications and redshifts for radio sources from the Wall & Peacock 2-Jy catalogue with declinations $\delta < +10°$, which bring the completeness of the optical identifications and redshifts to 97.9 and 91.5 per cent, respectively, for the southern part of the catalogue.

Key words: catalogues – galaxies: active – quasars: general – radio continuum: galaxies.

1 INTRODUCTION

The Wall & Peacock (1985, hereafter WP85) catalogue of radio sources provides an important set of 233 sources selected at 2.7 GHz and complete down to the flux density limit of 2 Jy. This catalogue covers the whole sky with the exception of the Galactic plane ($b \geq 10°$). Its importance is also that, being selected at higher frequencies compared to other surveys such as the 3CR, it is not biased against objects with a flat radio spectrum or an excess at centimetre wavelengths.

As Peacock & Wall (1982) have already shown, such objects, which are usually dominated by compact, self-absorbed components, represent a large fraction of the radio sources, particularly when high-redshift objects are considered. The study of the WP85 catalogue may be considered as complementary to what can be obtained using the 3CR catalogue, and hence is very important for a complete understanding of the characteristics of radio sources.

We are using the southern part ($\delta < +10°$) of this catalogue to study in detail the relationship between the radio and the optical properties of powerful radio sources. Because of the sparsity of good-quality data for these objects, we have devoted part of this project to collecting new spectroscopic and radio data.

The first results from these observations were presented in the first two papers of this series. In Tadhunter et al. (1993, hereafter Paper I), we presented the spectroscopic data of a complete subsample of the WP85 catalogue selected to have $\delta < +10°$ and $z < 0.7$, while Morganti et al. (1993, hereafter Paper II) presented new VLA and ATCA radio data for southern sources of the catalogue.

In order to ensure the completeness of the spectroscopic subsample, we have attempted to get good optical identifications and redshifts for all the WP85 southern sources. In this paper, we present these new identifications and redshifts, and review the status of the optical information for the southern sources of WP85.

2 SAMPLE SELECTION AND OBSERVATIONS

The WP85 catalogue contains 141 sources with $\delta < +10°$. Of these objects, 27 were known to have good identifications and spectroscopic redshifts larger than 0.7 in WP85, and, before we started our work, redshifts larger than 0.7 became available for another four sources, which were not re-observed by us. We set out to take spectra of all the other sources, except for nine objects with $z < 0.7$ which have very good-quality spectra in the literature (see Paper I for a list of these).

Table 1 lists all the 47 sources in the WP85 catalogue with $\delta < +10°$ and without spectroscopic redshifts in WP85, plus two objects (0043 − 12 and 0743 − 63) which had wrong spectroscopic redshifts in WP85. All these sources are the subject of this paper. WP85 have estimated redshifts for these objects based on the average relationship between redshift and V magnitude, separately for the radio galaxies and for the quasars. We shall discuss later the validity of this method for estimating redshifts.

The spectroscopic data of the sources for which we found $z < 0.7$ have already been presented in Paper I, since they form part of the complete spectroscopic subsample. These

†Presently at the Australia Telescope National Facility, CSIRO, Epping, Australia.

Table 1. New identifications and redshifts.

Object	α_{opt}(1950) h m s	δ_{opt}(1950) ° ′ ″	$\Delta\alpha_{rad-opt}$ ″	$\Delta\delta_{rad-opt}$ ″	ID	V mag	z	Refs.[a] opt,rad,V,z,FC
0008−42					EF	≳ 23		-,2,1,-,1
0022−42	00 22 15.36	−42 18 41.3	+1.1±0.6	+0.4±0.6	Q?	20.6		1,2,1,-,1
0023−26	00 23 18.96	−26 18 49.4	+0.0±0.6	−0.1±0.6	G	19.5	0.322	1,3,4,1,5
0039−44	00 39 46.89	−44 30 26.9	−0.6±2.7	+0.9±2.7[b]	G	18.5	0.346	1,27,4,1,1
0043−42	00 43 55.86	−42 24 14.6	[c]		G	16.0	0.116	1,2,4,1,7
0105−16	01 05 48.74	−16 20 20.4	+0.6±1.3	−0.7±1.3[b]	G	20.1	0.400	1,6,4,1,5
0114−21	01 14 26.00	−21 07 55.4	−0.7±0.6	+0.6±0.6	G	22.4		1,3,1,-,1
0117−15	01 17 59.66	−15 36 00.9	[c]		G	19.9	0.565	1,1,1,1,1
0157−31	01 57 58.41	−31 07 57.4	−1.4±0.6	+0.8±0.6	Q?	19.6		1,3,4,-,5
0213−13	02 13 12.35	−13 13 25.4	−1.5±1.2	+0.8±1.2	G	18.0	0.147	1,3,4,1,5
0235−19	02 35 24.76	−19 45 30.8	[c]		G	20.3	0.620	1,1,4,1,5
0252−71	02 52 26.49	−71 16 46.6	+0.8±0.9	−0.5±0.9	G	20.9	0.563	1,2,1,1,1
0347+05	03 47 07.07	+05 42 38.1	[c]		G	19.9	0.339?	1,1,1,1,1
0407−65					EF	≳ 21.5		-,2,8,-,1
0409−75	04 09 58.69	−75 15 04.8	[c]		G	20.8	0.694	1,2,1,1,1
0442−28	04 42 37.81	−28 15 22.6	[c]		G	17.4	0.147	1,1,4,1,5
0500+01	05 00 45.12	+01 58 54.2	+0.9±0.7	−0.4±0.7	G	21.4		1,3,9,-,9
0605−08	06 05 36.05	−08 34 19.2	+0.0±0.4	+0.0±0.4	Q	18.0	0.871	10,3,4,1,10
0743−67	07 43 22.20	−67 19 07.7	[c]		Q	16.4	1.510	1,2,4,1,11
0806−10	08 06 30.25	−10 18 50.5	+0.6±0.6	+0.3±0.6	G	17.8	0.110	1,3,4,1,12
0825−20	08 25 03.59	−20 16 28.2	+0.7±0.7	+0.5±0.7	Q	18.0	0.822	1,3,4,1,12
0834−19	08 34 56.02	−19 41 25.3	+0.7±0.7	−0.1±0.7	Q	21.9	1.032	1,3,9,1,9
0858−27	08 58 31.45	−27 56 33.5	+0.8±0.7	+0.4±0.7	Q	16.6	2.16	1,3,1,1,1
0859−25	08 59 36.40	−25 43 26.0	[c]		G	18.7	0.305	1,1,1,1,1
1005+07	10 05 22.04	+07 44 58.6	−0.3±0.6	+0.0±0.6	G	21.3	0.877	13,14,4,13,-
1015−31	10 15 53.41	−31 29 10.7	−0.4±0.6	−0.6±0.6	G?	20.2	1.346	1,3,4,1,5
1245−19	12 45 45.22	−19 42 57.2	+0.1±0.6	−0.3±0.6	Q	21.2	1.275	1,3,1,1,15
1306−09	13 06 02.04	−09 34 34.3	+0.7±1.0	+1.0±1.0	G	20.5	0.464	1,3,4,1,5
1308−22	13 08 57.36	−22 00 47.0	−0.1±1.0	+0.8±1.0	G?	21.5		1,3,4,-,5
1424−41	14 24 46.63	−41 52 57.1	+1.0±1.0	+2.4±1.0	Q	17.5	1.522	16,17,4,18,16
1518+04	15 18 44.70	+04 41 05.7	+0.0±0.8	−0.2±0.8	Q	22.8	1.294	19,3,4,1,19
1547−79	15 47 39.43	−79 31 43.0	[c]		G	19.7	0.482	1,2,1,1,11
1549−79	15 49 28.40	−79 05 17.5	−0.6±0.6	−0.2±0.6	G	18.8	0.150	1,2,4,1,20
1602+01	16 02 13.09	+01 25 56.4	[c]		G	20.5	0.463	1,1,4,13,20
1622−25	16 22 44.18	−25 20 51.6	−1.2±0.8	+0.0±0.8	Q	20.6	0.786	1,3,1,1,1
1733−56	17 33 21.48	−56 32 15.7	−0.1±1.0	−0.4±1.0	G	17.0	0.098	1,17,4,21,22
1740−51	17 40 27.21	−51 43 26.4	+0.6±0.7	−0.6±0.7	G	20.9		1,17,1,-,1
1741−03	17 41 20.58	−03 48 49.4	+0.6±0.5	+0.5±0.5	Q	18.5	1.054	23,24,4,18,23
1839−48	18 39 26.22	−48 39 23.0	−0.2±0.7	−0.1±0.7	G	16.5	0.112	1,3,4,1,25
1932−46	19 32 18.43	−46 27 20.8	[c]		G	19.0	0.231	1,2,1,1,1

Table 1 – *continued*

Object	α_{opt}(1950) h m s	δ_{opt}(1950) ° ′ ″	$\Delta\alpha_{rad-opt}$ ″	$\Delta\delta_{rad-opt}$ ″	ID	V mag	z	Refs.[a] opt,rad,V,z,FC
1938−15	19 38 24.60	−15 31 33.9	[c]		G	21.5	0.452	1,1,4,1,5
2008−06	20 08 33.66	−06 53 00.9	+0.6±0.8	−0.7±0.8	G	21.3		9,3,9,-,1
2032−35(1)	20 32 37.18	−35 04 34.9	[c]		G	22.6		1,26,1,-,1
2032−35(2)	20 32 37.33	−35 04 36.9	[c]		G	21.2		1,26,1,-,1
2106−41	21 06 19.40	−41 22 33.7	−0.1±0.7	+0.4±0.7	Q	20.0	1.055	5,24,4,18,5
2128+04	21 28 02.61	+04 49 04.5	+0.0±0.9	+0.0±0.9	G	23.5		19,3,19,-,19
2135−20	21 35 01.36	−20 56 03.5	−0.4±0.6	−0.2±0.6	G	19.4	0.635	1,3,4,1,5
2150−52			[c]		EF	≳ 21.5		-,2,8,-,5
2250−41	22 50 12.25	−41 13 44.4	[c]		G	19.9	0.310	1,2,1,1,1
2331−41	23 31 45.48	−41 41 59.9	[c]		G	21.1	0.907	1,27,1,1,1

[a]References for optical position, radio position, V magnitude, redshift and finding chart: (1) this work; (2) Duncan & Sproats (1992); (3) Morganti et al. (1993); (4) WP85; (5) Prestage & Peacock (1983); (6) Hunstead (1972); (7) Westerlund & Smith (1966); (8) limit of Southern Sky Survey J plate; (9) Fugmann et al. (1988); (10) Wills (1976); (11) Hunstead et al. (1971); (12) Bolton & Ekers (1966); (13) Spinrad et al. (1985); (14) Adgie, Crowther & Gent (1972); (15) Walter & West (1980); (16) Lü (1970); (17) Russell et al. (1992); (18) White et al. (1988); (19) Biretta et al. (1985); (20) Jauncey et al. (1989); (21) Hunstead et al. (1982); (22) White et al. (1987); (23) Véron et al. (1976); (24) Perley (1982); (25) Tritton & Whitworth (1973); (26) J. A. Peacock, private communication; (27) A. Burgess, private communication.

[b]Radio centroid position.

[c]The radio core is not detected. The 1950 positions of the radio lobes are

0043 − 42:	00 43 51.39	− 42 23 23.5,	00 44 00.60	− 42 25 06.1
0117 − 15:	01 17 59.35	− 15 36 06.2,	01 17 59.78	− 15 25 57.9
0235 − 19:	02 35 23.29	− 19 45 31.1,	02 35 25.94	− 19 45 37.1
0347 + 05:	03 47 06.64	+ 05 43 10.8,	03 47 07.38	+ 05 42 10.6
0409 − 75:	04 09 57.79	− 75 15 03.5,	04 09 59.12	− 75 15 06.7
0442 − 28:	04 42 36.01	− 28 14 41.5,	04 42 36.19	− 28 15 53.4
0743 − 67:	07 43 21.90	− 67 19 06.9,	07 43 23.71	− 67 19 12.2
0859 − 25:	08 59 35.18	− 25 43 14.2,	08 59 37.74	− 25 43 39.4
1547 − 79:	15 47 37.14	− 79 31 57.0,	15 47 42.77	− 79 31 26.0
1602 + 01:	16 02 12.50	+ 01 26 00.8,	16 02 13.23	+ 01 25 55.9
1932 − 46:	19 32 16.64	− 46 27 13.3,	19 32 19.56	− 46 27 24.2
1938 − 15:	19 38 24.31	− 15 31 32.8,	19 38 24.53	− 15 31 35.0
2032 − 35:	20 32 37.04	− 35 04 48.0,	20 32 37.28	− 35 04 32.9
2150 − 52:	21 50 47.67	− 52 04 16.9,	21 50 48.99	− 52 04 34.5
2250 − 41:	22 50 11.79	− 41 13 44.4,	22 50 13.27	− 41 13 46.4
2331 − 41:	23 31 44.80	− 41 42 05.3,	23 31 46.35	− 41 41 54.0

sources are discussed here only as far as identification and redshift are concerned.

The observations were performed in four runs, using the ESO 3.6-m telescope equipped with the EFOSC1 spectrograph and camera, and the ESO/MPI 2.2-m telescope with the Boller & Chivens spectrograph at La Silla, Chile. Table 2 gives information on the spectral observations not already presented in Table 1 of Paper I. More details on observational and data-reduction techniques are also given in Paper I.

3 RESULTS

The results on new identifications and redshifts are summarized in Table 1 and are discussed in more detail below.

3.1 New identifications

For the optical identification of the sources we used the most accurate radio positions available. These are usually VLA or ATCA positions of the core (Paper II) for which the accuracy ranges between 0.1 and 0.3 arcsec. The optical position was determined using sky maps extracted from the digitized Schmidt plates available at the Space Telescope Science Institute (Lasker et al. 1990). The astrometric information necessary to obtain good optical positions is provided in the headers of the maps themselves and was derived in the context of selecting guide stars for the *Hubble Space Telescope*. The fainter sources are not visible on the Schmidt plates: for these the optical positions were obtained by measuring the position of the optical counterparts on our CCD frames obtained with EFOSC1 relative to stars visible on the Schmidt scans. The accuracy of the optical positions is in general about 0.5 arcsec, and these positions agree, within the errors, with the estimated radio core positions (see Fig. 1 and Table 1).

The optical coordinates are given in Table 1, which also lists the radio-to-optical position offset, with errors including the radio and optical position errors, the V magnitude, mostly obtained from our own CCD frames, and the type of the optical counterpart: G for a galaxy, Q for a quasar, and EF for no optical counterpart, using the same criteria as WP85. The fact that the relative error on the radio-to-optical position offset is uniformly distributed and mostly smaller than one is an indication of the goodness of our identifications. Individual cases are discussed in the next section.

In Fig. 2, we show the finding charts for the new identifications and for the objects that were lacking a good finding chart in the literature.

3.2 New redshifts

We have obtained new spectroscopic redshifts for 31 objects (see Table 1), including two (0043−42 and 0743−67) that were listed with wrong redshifts in WP85.

Fig. 3 shows our spectra for the sources with $z>0.7$, and Table 3 lists the strongest emission lines for the same objects. This complements the information for objects with $z<0.7$ given in Paper I.

3.3 Objects without identification or redshift

Three objects are still lacking optical identifications. We do not have new CCD frames for two of them: therefore the lower limit to the magnitude of their optical counterpart is the limit of the UK Schmidt Survey plates. On the other hand, the limit we give in Table 1 for the optical counterpart of 0008−42 is that of our CCD frame.

Table 2. Details of the spectral observations.

Object	Grism*	Slit width arcsec	Exp. time min	Period
0022 − 42	B300	2.0	20	Dec. 89
0114 − 21	B300	2.0	20	Dec. 89
0347 + 05	B300,R300	2.0,2.0	20,30	Dec. 89
0500 + 01	B300,R300	2.0	30,30	Dec. 89
0605 − 08	B300	1.5	2x15	March 89
0743 − 67	B300,R300	2.5	2x10,5	March 89
	B300	5	3	
	R300	1.5,5	10,0.5	
0825 − 20	R300	1.5,5	20,5	March 89
0834 − 19	R300,B300	1.5	2x20,20	March 89
0858 − 27	B300	2.5,5	20,5	March 89
	R300	1.5,5	20	
1015 − 31	R300	1.5	2x20	March 89
	B300	1.5	2x20	
1245 − 19	R300	1.5	2x20	March 89
1518 + 04	B300,R300	1.5	40,40	April 89
1622 − 25	B300	1.5,3	2x20,5	April 89
	R300	2.0	30	March 93
1740 − 51	B300	1.5	30,15	April 89
2008 − 06	R300,B300	2.0	10,10	July 90
2032 − 35	R300,B300	3.0	10,10	July 90
2128 + 04	R300	3.0	10	July 90
2331 − 41	R300	5.0	5	July 90

*Wavelength range for the grisms: B300 = 3600–7000 Å; R30 = 5600–9900 Å.

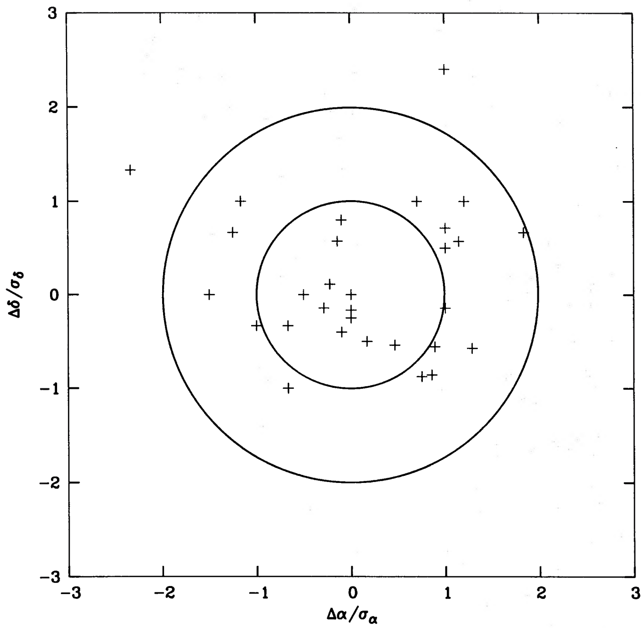

Figure 1. A plot of the difference between the radio and optical coordinates divided by the combined radio and optical positional errors. The circles represent the 1σ and 2σ confidence limits.

The additional nine objects for which we have failed to identify recognizable features in our optical spectra (we took spectra of all the identified sources listed in Table 1, except 1308 − 12) are fainter than $V = 19.6$ for quasars and $V = 20.9$ for radio galaxies, and therefore they should have redshifts larger than 0.7, based on the observed correlation between redshift and apparent magnitude for radio galaxies and quasars (see Section 5 and WP85), except for 1740 − 51, for which we estimate a redshift of 0.66 (this object actually has some faint, unidentified emission lines). Therefore, given also the other indications that these objects are distant already mentioned in Paper I, it appears likely that the majority of the unknown redshifts are high, and that our spectroscopic sample with $z < 0.7$ (Paper I) is mostly complete, once 0347 + 05 is added to it.

4 COMMENTS ON INDIVIDUAL OBJECTS

0008 − 42. This compact, steep-spectrum radio source remains unidentified, since our deep V image does not show any object down to $V \sim 23.0$ within 3σ of the new accurate radio position (Duncan 1992) (Fig. 2).

0022 − 42. We identify this compact, steep-spectrum source with a faint stellar object (Fig. 2). Its spectrum shows a faint red continuum without clear emission, but with one unidentified absorption line at 5415 Å.

0039 − 44. We identify this double-lobed source with a galaxy (Fig. 2), which probably corresponds to the identification of Savage (1976), although it is not visible in her finding chart. Its spectrum has strong emission lines (Paper I) at $z = 0.346$.

0043 − 42. This radio galaxy was identified by Westerlund & Smith (1966) and is located precisely between the radio lobes in the AT map of Duncan & Sproats (1992). Our spectrum shows absorption and weak emission lines (Paper I) at a redshift of 0.116, while Whiteoak (1972) gave an absorption redshift of 0.0526.

0105 − 16. This galaxy identified by Moseley et al. (1970) and Prestage & Peacock (1983) is located very close to the central position between the lobes of the radio map presented in Paper II. Our spectra show absorption and strong emission lines (Paper I) at $z = 0.400$.

0117 − 15. This double-lobed source is identified with a galaxy situated very close to the line joining the radio lobes (Fig. 2). It has a compact nucleus and a jet-like extension up to 5.5 arcsec to the north-east, aligned with the radio axis. Our spectrum was taken with the slit in position angle PA = 48° and shows that the nucleus has a faint continuum and strong emission lines (Paper I), while the extension has only line emission, stronger than in the nucleus and redshifted by about 650 km s^{-1}. Prestage & Peacock (1983) had two candidate identifications, of which only one is seen in our CCD frame. Fugmann, Meisenheimer & Rözer (1988) have also split the object in two.

0157 − 31. The tentative identification given by Prestage & Peacock (1983) coincides with the core of this triple source (Paper II) and is therefore confirmed.

0213 − 13. The galaxy given as an uncertain identification by Prestage & Peacock (1983) is within 1.5 arcsec of the position of the weak core of this triple radio source and is therefore the definite identification. The galaxy has strong narrow emission lines (Paper I) at a redshift of 0.147.

0252 − 71. The identification of Savage et al. (1977) is resolved into two objects in our CCD frame (Fig. 2): the fainter one to the north-west is slightly resolved and is closer to the accurate radio position (Duncan 1992). Our spectrum across both objects shows that the brighter one is a Galactic star. The other object has clear emission lines (Paper I) at a redshift of 0.563 and is therefore the definite identification.

0347 + 05. A faint galaxy lies on the line joining the radio lobes (accurate position from Paper II) close to the mid-point (Fig. 2). It is the same identification as proposed by Fugmann et al. (1988), although on their finding chart the object is not separated from the stellar one to the south-west, while the identification suggested by Prestage & Peacock (1983), i.e. the bright stellar object close to the northern lobe, is probably wrong. Our blue and red spectra of the galaxy show a red continuum and faint emission lines, which we tentatively identify with [O II] 3727, broad Hβ, [O III] 5007 (the two latter lines are visible on both our spectra) and broad Hα at a redshift of 0.339. No features are visible on the continuum of the other object. We consider the galaxy to be the most likely identification, although a deeper spectrum is needed to confirm its redshift.

0407 − 65. The identification proposed by Prestage & Peacock (1983) is not compatible with the new accurate position of this compact radio source (Duncan 1992). No object is visible within 3σ of this position on the digitized Schmidt plate obtained from the Guide Star Project of the StScI (Fig. 2). This source therefore remains unidentified.

0409 − 75. We identify this source with a galaxy, possibly resolved into two components in our CCD frame (Fig. 2). It is not clear if the galaxy is either of the two candidates proposed by Prestage & Peacock (1983). Our blue and red spectra show a red continuum with emission lines (Paper I) at a redshift of 0.694. The [O II] 3727 line is clearly extended. The stellar object to the south-east has a faint red continuum.

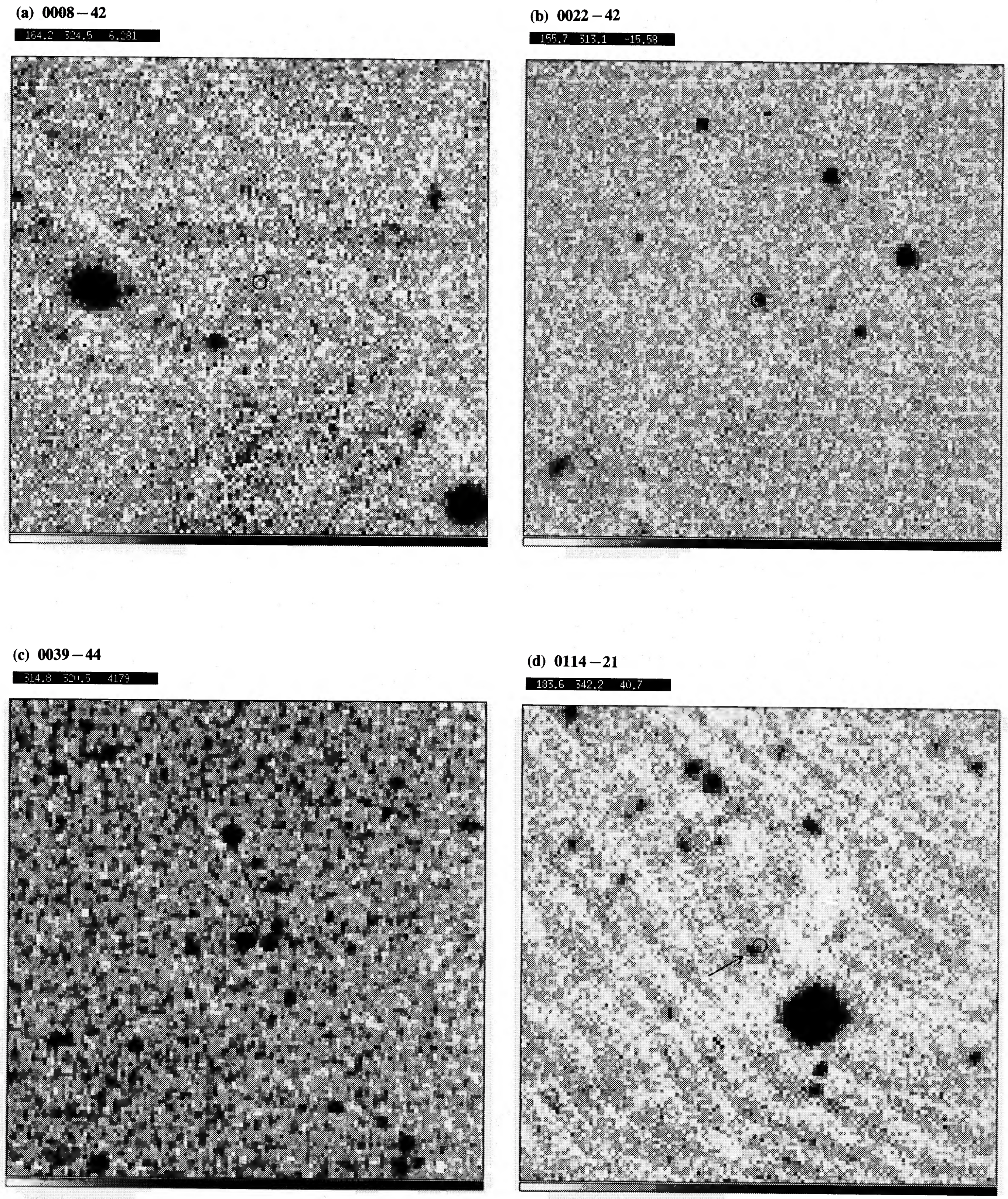

Figure 2. Finding charts for the sources lacking a good finding chart in the literature. North is to the top and east to the left. The field side corresponds to 86 arcsec, except for 0039 − 44, 0407 − 65 and 2331 − 41 where it is 217 arcsec. The circles indicate the positions of the radio core or of the lobes. The radii of the circles correspond to twice the combined radio–optical rms position errors. The arrows point to the optical counterparts in the ambiguous cases.

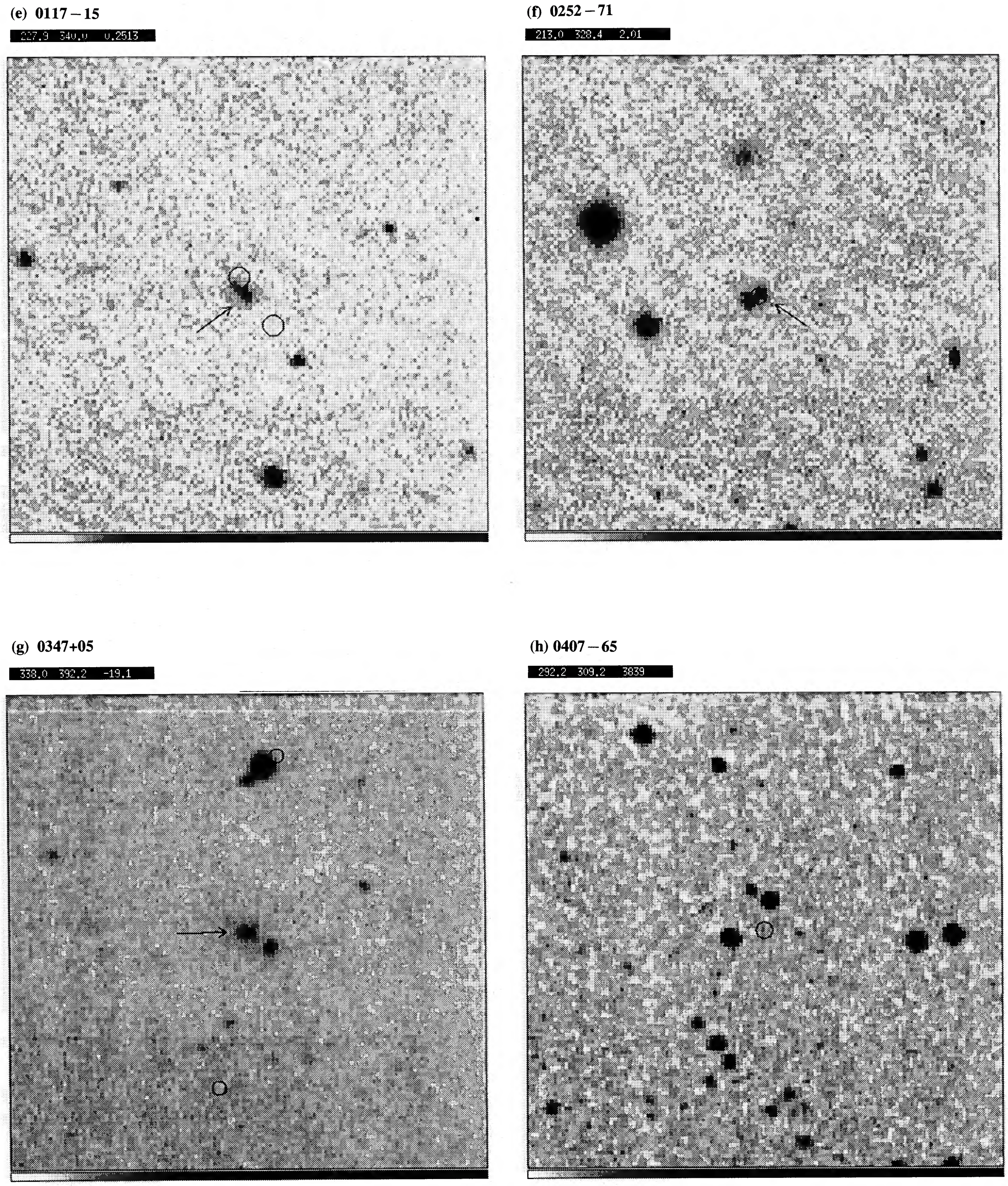

Figure 2 – *continued*

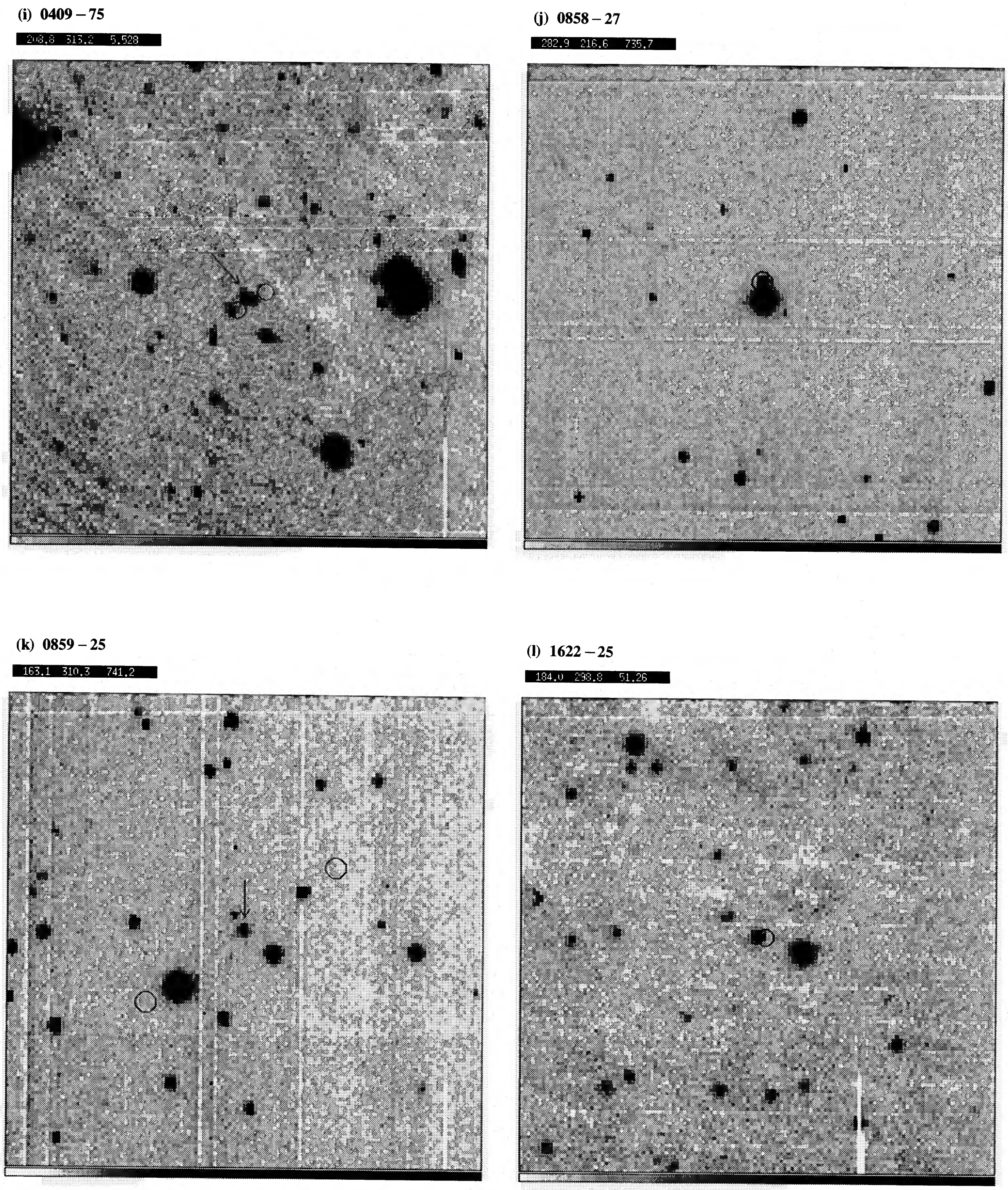

Figure 2 – *continued*

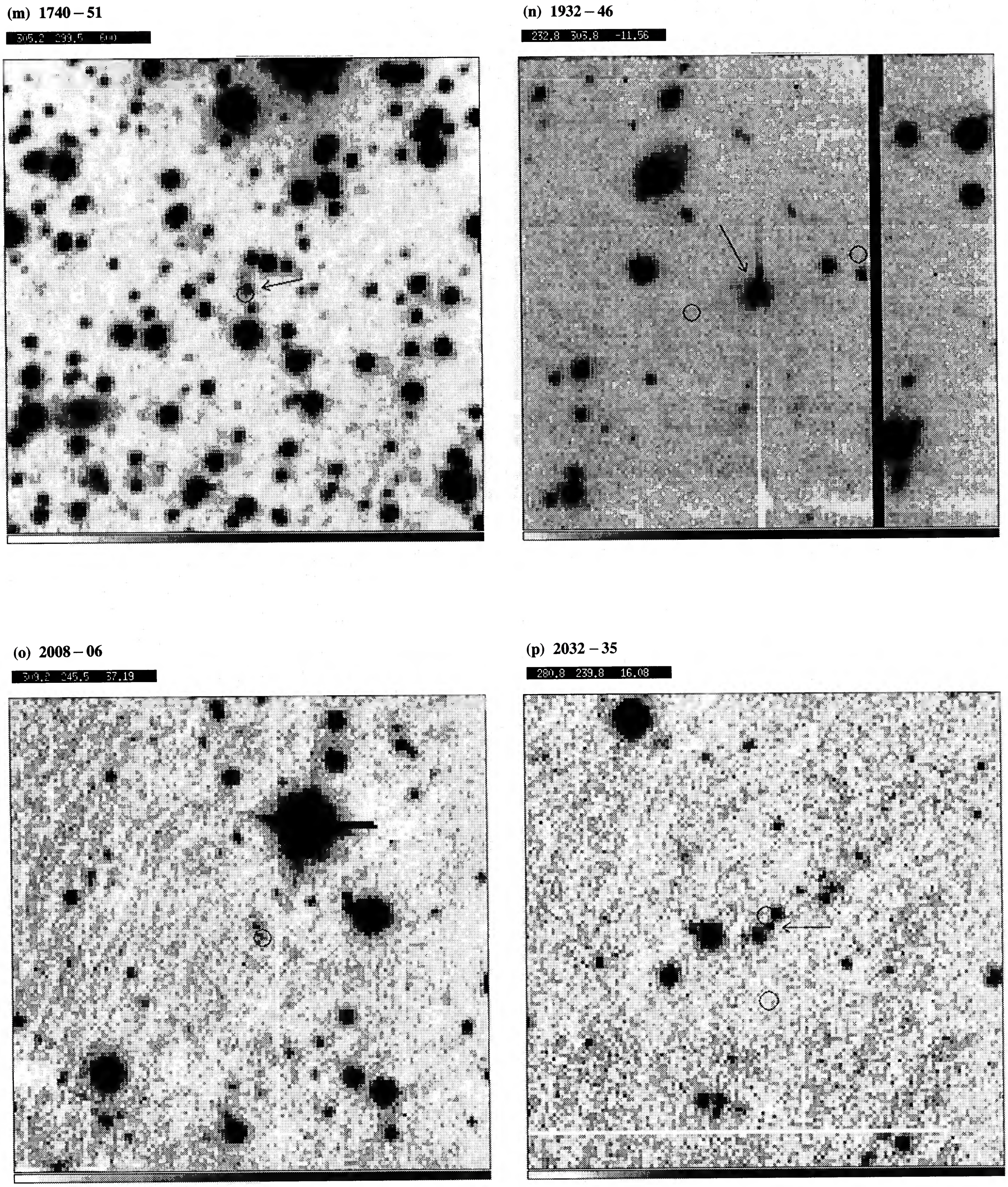

Figure 2 – *continued*

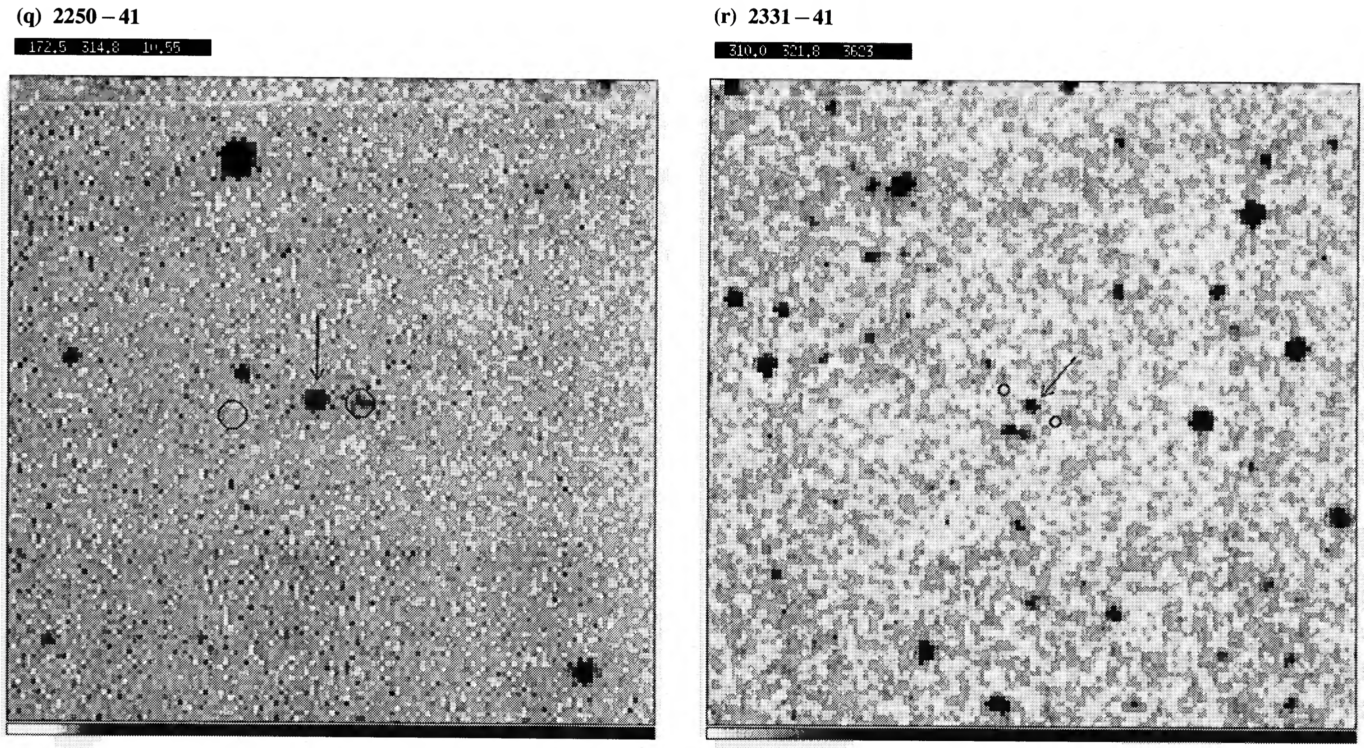

Figure 2 – *continued*

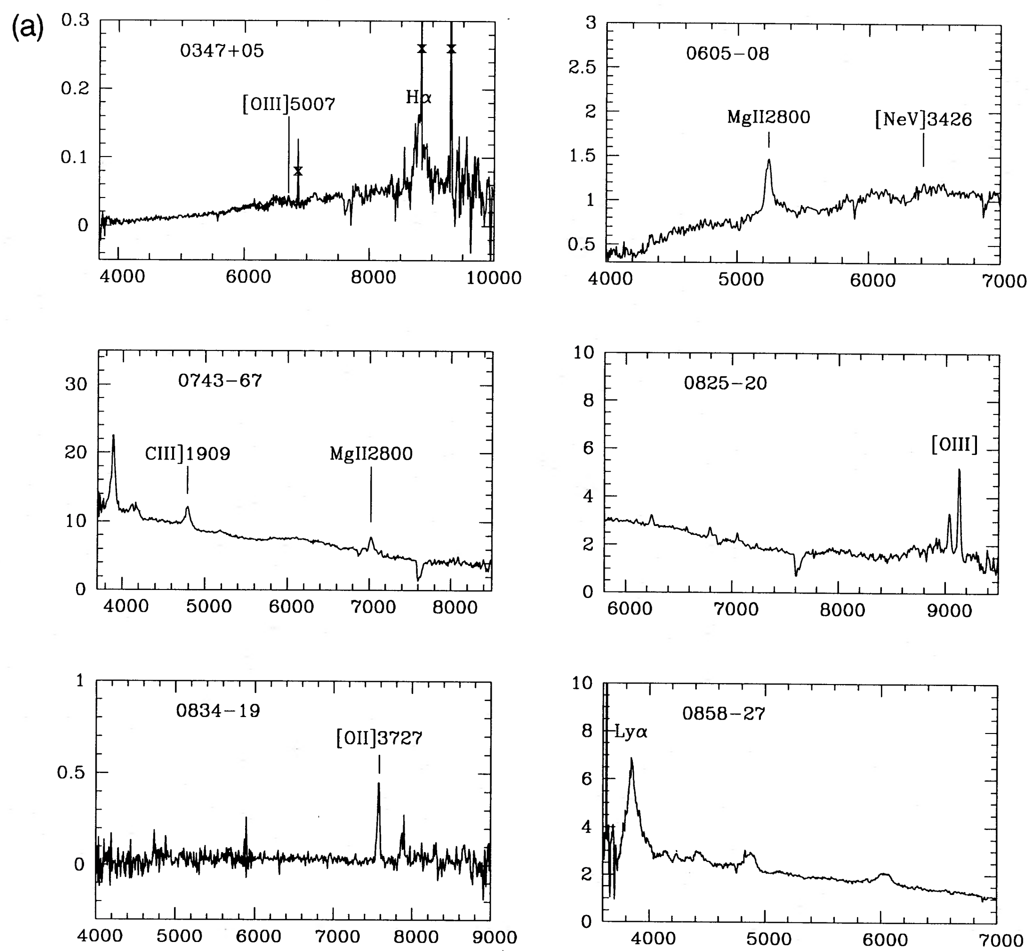

Figure 3. Spectra of the observed objects with $z > 0.7$ and of 0347 + 05. Cosmic ray signatures are marked with x, and residual sky features are marked with s.

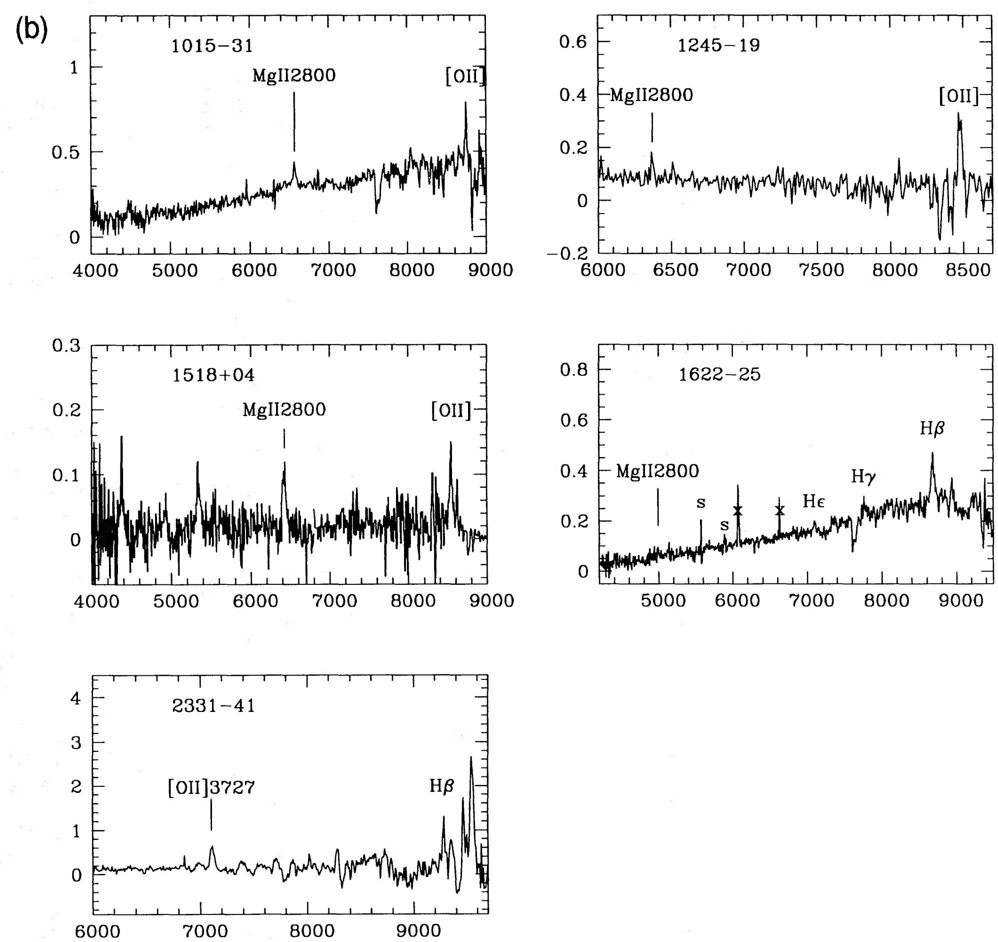

Figure 3 – *continued*

0500 + 01. This compact radio source was identified by Fugmann et al. (1988). Our CCD frame shows their object 1 to be slightly resolved, and its spectrum has a faint red continuum with possible emission lines at 5910 and 6400 Å.

0605 − 08. The accurate VLA position (Paper II) coincides with that of the blue stellar object identified by Wills (1976). Its spectrum shows broad Mg II 2800, already detected by Wills & Wills (1976) and [Ne V] 3426 at $z = 0.871$ (Fig. 3 and Table 3).

0743 − 67. This quasar is listed with a wrong redshift of 0.395 in the WP85 catalogue. Our spectrum (Fig. 3 and Table 3) shows typical quasar lines (C IV 1550, He II 1640, C III 1909 and Mg II 2800) at a redshift of 1.512 coincident with the one found by Bergeron & Kunth (1984).

0806 − 10. This radio galaxy has strong emission lines (Paper I) at a redshift of 0.110. The emission lines are extended by about 7 arcsec in the direction of the radio axis (PA = 19°).

0825 − 20. The optical identification of Bolton & Ekers (1966) is stellar on Schmidt plates. Our red spectrum shows strong emission lines of Ne V] 3426, [O II] 3727, [Ne III] 3869 and [O III] 4959, 5007 and possibly broad Hβ (Fig. 3 and Table 3) at a redshift of 0.822.

0834 − 19. We identify this compact steep-spectrum source with a faint stellar object – object 1 of the finding chart of Fugmann et al. (1988). Its spectrum has clear emission lines of [Ne V] 3426, [O II] 3727 and [Ne III] 3869 (Fig. 3 and Table 3).

0858 − 27. Radivich & Kraus (1971) identified this compact steep-spectrum source with a stellar object 3.6 arcsec to the north of a bright star (Fig. 2). It has a typical quasar spectrum (Fig. 3 and Table 3) with a redshift of 2.16.

1015 − 31. This compact steep-spectrum source was identified by Prestage & Peacock (1983) and appears stellar on Schmidt plates. Its spectrum shows a red continuum and emission lines of [C III] 1909, Mg II 2800, [Ne V] 3424 and [O II] 3727 at a redshift of 1.346 (Fig. 3 and Table 3).

1245 − 19. This object, identified by Walter & West (1980), appears stellar on our CCD frame. Its spectrum has emission lines of Mg II 2800 and [O II] 3727 at a redshift of 1.273 (Fig. 3 and Table 3).

1518 + 04. This compact, steep-spectrum source was identified with a faint stellar object by Biretta, Schneider & Gunn (1985). Our spectrum shows broad emission lines of C III 1909, C II 2326 and Mg II 2800 at a redshift of 1.296 (Fig. 3 and Table 3).

1547 − 79. This radio galaxy was identified by Hunsted (1971). It is indeed located between the radio lobes of the new AT map by Duncan & Sproats (1992), and it has clear emission lines (Paper I) at $z = 0.482$.

Table 3. Line fluxes.

Object	Line	Wavelength Å	Flux 10^{-16}erg cm^{-2} s^{-1}
0605−08	MgII2800	5236.95	36.74
	[NeV]3426	6414.01	2.3:
0743−67	CIV1550	3887.97	560.06
	HeII1640	4113.95	51.45
	CIII]1909	4784.48	193.02
	MgII2800	7021.73	92.49
0825−20	[NeV]3426	6242.17	13.36
	[OII]3727	6793.76	12.72:
	[NeIII]3869	7048.15	8.44
	[OIII]5007	9125.58	104.86
0834−19	[NeV]3426	6969.60:	1.82
	[OII]3727	7574.92	15.98
	[NeIII]3869	7860.49:	3.60:
0858−27	Lyα	3851.91	374.99
	SiIV/OIV	4425.53	31.37
	CIV1550	4865.53	57.37
	CIII]1909	6022.43	47.57
1015−31	CIII]1909	4470.53	2.98
	MgII2800	6563.79	4.67
	[NeV]3426	8042.24	2.84:
	[OII]3727	8747.12	5.54
1245−19	MgII2800	6368.9:	1.89:
	[OII]3727	8476.08	7.20
1518+04	CIII]1909	4378.85	3.62
	CII]2326	5335.36	1.70:
	MgII2800	6423.45:	4.1:
	[OII]3727	8545.12	3.80
1622−25	MgII2800	4993.62	6.08:
	Hϵ	7100.12	1.9:
	Hβ	8684.95	10.0:
2331−41	[OII]3727	7112.43	3.94
	[NeIII]3869	7390.12	18.9
	Hβ	9285.17	31.24
	[OIII]5007	9550.32	25.43

1622 − 25. This compact radio source is identified with a stellar object (Fig. 2). Its spectrum has a faint red continuum with emission lines of Mg II 2800, Hϵ, Hδ, Hγ, Hβ and [O III] 5007 (Fig. 3 and Table 3) at $z = 0.786$. The brighter object to the south-west (marked in the finding chart of Prestage & Peacock 1983) is a Galactic star with Balmer absorption lines.

1740 − 51. The only object within twice the combined radio-optical position error (rms) from the new accurate radio position (Duncan 1992) of this compact, steep-spectrum source is a faint galaxy extended up to about 5 arcsec towards the north. Its spectrum shows a very red continuum with possible emission lines at 5367, 5870 and 5962 Å. No features are visible in the spectrum of the faint stellar object 3.5 arcsec south of the galaxy, while the brighter object further south (object b in the finding chart of Prestage & Peacock 1983) is a Galactic F star. Although the field is crowded, we consider the galaxy to be a secure identification.

1839 − 48. The galaxy identified by Tritton & Whitworth (1973) coincides with the new accurate radio position (Paper II), while the radio position of Large et al. (1981) is off by more than 10 arcsec. The galaxy spectrum has several absorption lines typical of early-type galaxies at a redshift of 0.115, but no emission lines (Paper I). The galaxy is the brightest member of a group. The companion galaxy at 14 arcsec to the south-west (PA = 221°) has a double nucleus and absorption lines at $z = 0.116$.

1932 − 46. We identify this double-lobed source with a galaxy situated precisely between the radio lobes, closer to the eastern one (Fig. 2). Our spectrum taken with the slit in PA = 90° shows strong emission lines (Paper I) extended toward the east up to 8 arcsec from the nucleus. A separated emission-line region is clearly detected in both our long-slit spectra at about 19 arcsec east of the nucleus at the same redshift (Table 3). This region extends by at least 4 arcsec along the slit and shows no continuum. We remark that the region is fairly well aligned with the radio axis, but is located beyond the eastern radio lobe. The identification with the galaxy was rejected by Prestage & Peacock (1983), possibly because of the inaccurate radio position that they used.

1938 − 15. We identify this double-lobed source with a faint galaxy located between the radio lobes. This object is labelled C in the finding chart of Prestage & Peacock (1983). They rejected this identification because of the inaccurate radio position that they used. The galaxy has strong emission lines (Paper I) at a redshift of 0.452.

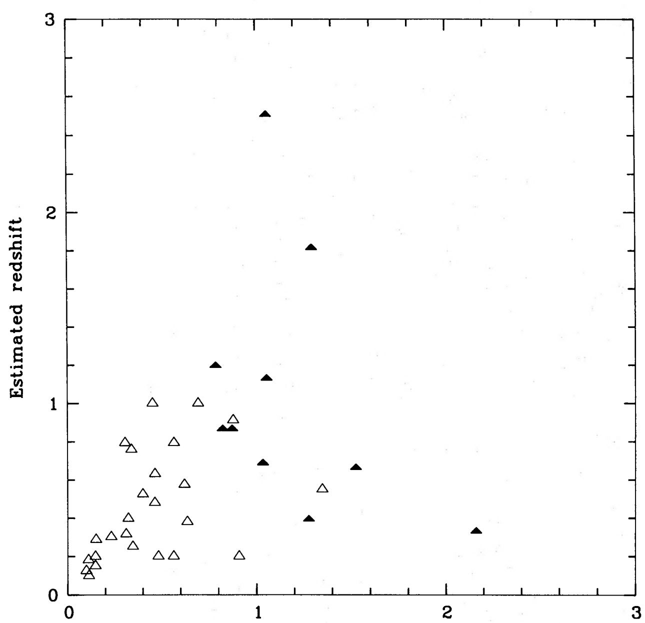

Figure 4. A comparison of our new spectroscopic redshifts with those estimated from the Hubble diagram by WP85 for radio galaxies (empty symbols) and quasars (filled symbols).

2008 − 06. This faint galaxy was identified by Fugmann et al. (1988) and has a strongly elongated multicomponent structure extending by up to 6 arcsec in PA = 26°. The compact, steep-spectrum source coincides with the southernmost component (Fig. 2).

2032 − 35. The most likely identification for this double-lobed source is the faint diffuse object (marked with an arrow in Fig. 2, object 1 in Table 1) closest to the line joining the radio lobes (accurate position from Peacock, private communication). The brighter object at about 3 arcsec to the south-east (object 2 in Table 1) is also a possible identification. If either of these two identifications is correct, the radio source would be highly asymmetric. The identification given by Prestage & Peacock (1983) is not visible on our CCD frame.

2150 − 52. No object is detected on the UK Schmidt *J* plate for the Southern Sky Survey between the radio lobes (coordinates from Duncan & Sproats 1992) of this source (see also Prestage & Peacock 1983). We have no CCD frame for this field. WP85 list as a tentative identification a faint object (G?) with $V = 22.2$, possibly based on their unpublished CCD data, but do not list the optical coordinates.

2250 − 41. We identify this double-lobed source with a galaxy situated between the radio lobes (Fig. 2). Its spectrum has a faint red continuum and strong, narrow emission lines (Paper I) at a redshift of 0.310. The fainter extended source at 7 arcsec to the west, coinciding with the western lobe, has strong emission lines at the same redshift and no continuum (Table 3). The magnitude given in Table 1 refers to the integrated light of both sources. Hunstead (1971) identified the radio source with the emission line region to the west.

2331 − 41. This double-lobed source was identified by Lü (1970) with a faint galaxy which is located between the radio lobes (coordinates from A. Burgess, private communication) (Fig. 2). Its spectrum has narrow emission lines of [Ne v]

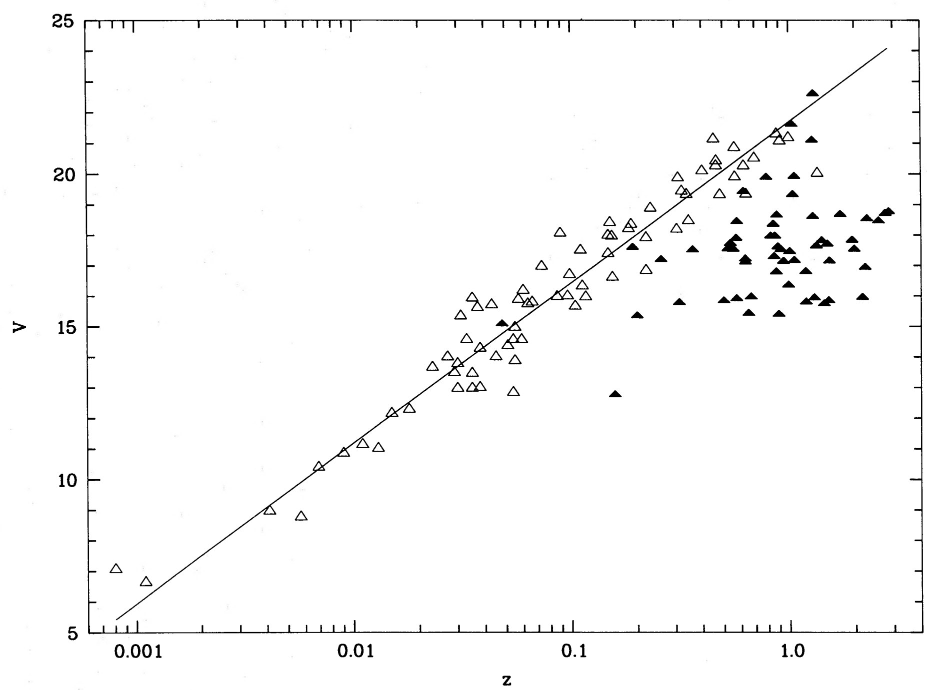

Figure 5. The Hubble diagram for the radio galaxies (empty symbols) and the quasars (filled symbols) in the southern part of the WP85 catalogue.

3426, [O II] 3727, [Ne III] 3869, Hγ(?), Hβ and [O III] 4959, 5007 at a redshift of 0.907 (Fig. 3 and Table 3).

5 DISCUSSION

This work brings the completeness of the optical identifications and redshifts for the 141 sources in the southern part of the WP85 catalogue to 97.9 and 91.5 per cent, respectively, close to what was obtained with heroic efforts in the early 1980s for the 3CR catalogue (Spinrad et al. 1985).

Our new spectroscopic redshifts enable us to assess the reliability of evaluating redshifts from the Hubble diagram (WP85): Fig. 4 shows a plot of the new spectroscopic redshifts versus the redshifts estimated from V magnitudes by WP85. It is clear that large errors have been made by WP85 for a number of objects, both radio galaxies and quasars.

Fig. 5 shows the Hubble diagram for the southern part of the WP85 catalogue, using our new redshifts and magnitudes, and improved magnitudes obtained from Peacock & Wall (1989, private communication). The V magnitudes plotted in Fig. 5 have been corrected for the Galactic extinction, evaluated from the maps of Burstein & Heiles (1982) assuming that $A_V = 3.0 \times E(B-V)$. It is clear that the diagram for the radio galaxies has a small spread: therefore most of the errors in the WP85 redshift estimates for these objects are due to incorrect V magnitudes, while the method of using the Hubble diagram is substantially valid for radio galaxies.

The continuous line in Fig. 5 represents the best fit of the data for radio galaxies:

$$\log z = 0.19(\pm 0.01)\, V - 4.13(\pm 0.31).$$

This relation is only slightly different from the previous one presented by WP85. For quasars the correlation between z and V is hardly visible in Fig. 5: therefore it cannot be used for a reliable estimate of the redshift.

ACKNOWLEDGMENTS

We thank John Peacock for communicating unpublished data, Stefano Cristiani for help with the redshift of 1622 − 25, and Dave Burstein for providing a computer-readable version of the Galactic extinction maps.

This work was based on observations obtained at the European Southern Observatory, La Silla, Chile.

REFERENCES

Adgie R. L., Crowther J. H., Gent H., 1972, MNRAS, 159, 233
Bergeron J., Kunth D., 1984, MNRAS, 207, 263
Biretta J. A., Schneider D. P., Gunn J. E., 1985, AJ, 90, 2508
Bolton J. G., Ekers J., 1966, Aust. J. Phys., 19, 559
Burstein D., Heiles C., 1982, AJ, 87, 1165
Duncan R. A., 1992, 'ATCA Calibrator List', ATNF Internal Doc., Australian Telescope National Facility, CSIRO
Duncan R. A., Sproats L. N., 1992, Proc. Astron. Soc. Aust., 10, 16
Fugmann W., Meisenheimer K., Röser H.-J., 1988, A&AS, 75, 173
Hunstead R. W., 1971, MNRAS, 152, 277
Hunstead R. W., 1972, MNRAS, 157, 367
Hunstead R. W., Lasker B. M., Mintz B., Smith M. G., 1971, Aust. J. Phys., 24, 601
Hunstead R. W., Durdin J. M., Little A. G., Reynolds J. E., Kesteven M. J. L., 1982, Proc. Astron. Soc. Aust., 4, 447
Jauncey D. L., Savage A., Morabito D. D., Preston R. A., 1989, AJ, 98, 54
Large M. I., Mills B. Y., Little A. G., Crawford D. F., Sutton J. M., 1981, MNRAS, 194, 693
Lasker B. M., Sturch C. R., McLean B. J., Russell J. L., Jenkner H., Shara M. M., 1990, AJ, 99, 2019
Lü P. K., 1970, AJ, 75, 1164
Morganti R., Killeen N. E. B., Tadhunter C. N., 1993, MNRAS, 263, 1023 (Paper II)
Moseley G. F., Brooks C. C., Douglas J. N., 1970, AJ, 75, 1015
Peacock J. A., Wall J. V., 1982, MNRAS, 198, 843
Perley R. A., 1982, AJ, 87, 859
Prestage R. M., Peacock J. A., 1983, MNRAS, 204, 355
Radivich M. M., Kraus J. D., 1971, AJ, 76, 683
Russell J. L. et al., 1992, AJ, 103, 2090
Savage A., 1976, MNRAS, 174, 259
Savage A., Bolton J. G., Wright A. E., 1977, MNRAS, 179, 135
Spinrad H., Djorgovski S., Marr J., Aguilar L. A., 1985, PASP, 97, 932
Tadhunter C. N., Morganti R., di Serego Alighieri S., Fosbury R. A. E., Danziger I. J., 1993, MNRAS, 263, 999 (Paper I)
Tritton K. P., Whitworth D. P. D., 1973, MNRAS, 165, 253
Véron M. P., Véron P., Adgie R. L., Gent H., 1976, A&A, 47, 401
Wall J. V., Peacock J. A., 1985, MNRAS, 216, 173 (WP85)
Walter H. G., West R. M., 1980, A&A, 86, 1
Westerlund B. E., Smith L. F., 1966, Aust. J. Phys., 19, 181
White G. L., Batty M. J., Bunton J. D., Brown D. R., Corben J. B., 1987, MNRAS, 227, 705
White G. L., Jauncey D. L., Savage A., Wright A. E., Batty M. J., Peterson B. A., Gulkis S., 1988, ApJ, 327, 561
Whiteoak J. B., 1972, Aust. J. Phys., 25, 233
Wills B. J., 1976, AJ, 81, 1031
Wills D., Wills B. J., 1976, ApJS, 31, 143